Military Technical College
Kobry Elkobbah,
Cairo, Egypt

2nd International Conference
on Electrical Engineering
ICEENG 99

A PROTOCOL FOR CORRECTION OF MACHINE DEPENDENCY FOR ULTRASOUND IMAGING

Yasser M. Salman. B.Sc.*, Ahmed M. Badawi** Ph.D., S.E. Shouman*** Ph.D.

ABSTRACT

When analyzing ultrasound images, the processed data depends strongly on the settings of the equipment. So, the overall gain, Time-Gain-Compensation(TGC) , Diffraction and Focusing, pre-and post processing of the gray levels, all play a role in the estimation of the texture parameters. To correct for these dependencies, we used images from tissue mimicking phantom with the same settings of the ultrasound equipment as during the clinical procedure. The acoustic properties of the phantom have been estimated in the device developed for acoustic microscopy. Steps of image correction are: Look Up Table (LUT) Correction, Time-Gain-Control Correction and Focusing and Diffraction Correction.

KEY WORDS

image correction, ultrasound images, texture parameters, Look Up Table (LUT) Correction, Time-Gain-Control Correction and Focusing and Diffraction Correction.

*Graduate student, Dpt. of Electronic Eng., M.T.C, Kobry Elkobbah, Egypt.
** Ph.D., Dpt. Of Biomedical Eng., Faculty of Engineering,Guiza, Egypt.
***Associate professor, Dpt. of Electronic Eng., M.T.C, Kobry Elkobbah, Egypt.

1.INTRODUCTION

The use of ultrasonorgaphy as an imaging modality has become widely spread because of its ability to visualize main organs with no deleterious effects. The basic idea of ultrasonic imaging is to send the fine beam of ultrasonic waves through the human tissues and then receive the characteristic echo reflections from the internal body structure to form the ultrasound image. The different gray levels of this image represent the acoustic properties of the human tissues such as attenuation of acoustic waves, speed of sound and acoustic impedance of the different body structures. All these factors contribute to the shape and intensity of the returned waves according to the underlying tissue properties and hence, this fact is the basis for the use of ultrasonography as an imaging technique. The main limitation for ultrasound is its inherent inability to visualize air-containing or bony structures.[1]

Conventional gray scale B-mode ultrasound is widely applied and useful diagnostic tool in the management of liver diseases. Nevertheless its operator dependency leading to considerable observer variation, and varying figure for its diagnostic accuracy are well documented in the literature [2]. Visual criteria for diagnosing diffused liver diseases are in general confusing and highly subjective because they depend on the sonograoher to observer certain textural characteristic from the image and compare them to those developed for different pathologies to determine the type of the disease. An example for these features is texture homogeneity. Its presence or absence can be widely debated between different experienced sonographers. Another feature is texture echogenicity which can be a matter of argument in marginal cases. Moreover, some of the diseases are highly similar in their diagnostic criteria, which tend to confuse the event .The visual criteria provides low diagnostic accuracy (around 70 %) [2-3]. Therefore the physicians may have to use further invasive methods such as pathology investigation of ultrasonically guided needle biopsy. Although this technique is considered to be the golden test for diagnosis, it has the disadvantage of being invasive and more importantly, it may cause a great risk of cancer spread if it cuts through a localized cancer area [5-8] quantitative tissue characterization has been described in the literature using tissue backscattering and attenuation measurements. Researchers have used pattern recognition to classify different diffuse liver pathologies [3-8]. The major problem in the echographic diagnostics , which is almost completely neglected, is the dependence of the tissue texture on the performance characteristics of the equipment[9-11].The problem here that the processed data depends strongly on the setting of the equipment . So, the Time-Gain-Compensation(TGC) , Diffraction and Focusing, pre-and post processing of the gray levels, all play a role in the estimation of the texture parameters.

2.DATA ACQUISITION SYSTEMS AND SYSTEMS SETTINGS

I) Data acquisition systems

The data acquisition systems and aTL machine system were developed at *Dr. Abou-Bakr's Youssef Clinic and Kasr Elaini medical school Hospital, Cairo, Egypt.*

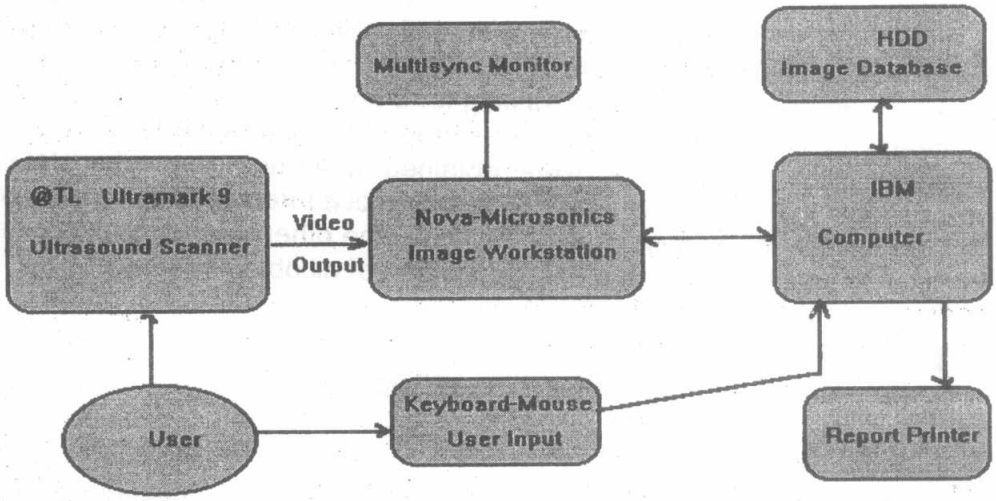

Fig.1. Block Diagram for Developed System at Kasr-Elaini medical school

In the system shown in fig.1., the video output of an aTL Ultramark model 9 ultrasound machine was connected to a Nova-Microsonics workstation for image acquisition.The cineloop images are captured at a rate of 30 frames/sec for fully inspired controlled limb movement and controlled inspiration patients. The images are captured with grey-level resolution of 8 bits/pixel at 3.5 MHz .

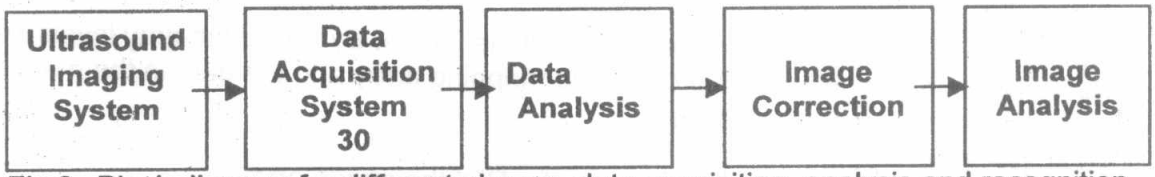

Fig.2. Block diagram for different phases, data acquisition, analysis and recognition.

The Images are then reformatted from the DEF format of the Nova-Microsonics workstation and analyzed at a P-II-300 computer machine. The axial resolution at this setting was 32 pixel/cm and lateral resolution 26 pixels/cm for the system settings. A software was developed on this system to allow the sonographer to define the region of interest in the image for tissue characterization and for further motion and elasticity analysis (WINDOWS95 operating systems).

II) Systems settings

To obtain a reproducible results, the following parameters were standardized for all tissue characterization procedures [6-8] for the system:

1. *Ultrasound machine settings:* e.g., TGC, FOCUS, and ZOOM controls, which can change the overall image gain and produce zooming effects and hence they can deviate the image statistics in an unpredictable way. Moreover, the frequency of ultrasound waves used must be the same for all the patients since the attenuation of ultrasonic waves depends mainly on this frequency. The diffraction and focussing for system were corrected using two different tissue mimicking AIUM phantoms at 0.5 dB/cm.MHz, the other at 0.7 dB/cm.MHz.
2. *Region-of-interest (ROI) size and shape:* to obtain a reliable statistics, the number of pixels in the region of interest must be at least a thousand pixels (4cm * 4cm, 128*128 pixels). A practical ROI size must be taken to cover the all texture in the

image and far from edges. Also, the square shape of the region should be maintained during all procedures, and for mapping the polygon region should be maintained to be more flexible to select the ROI.

3. *Fasting condition of the patient:* fasting for 8 hours before the scan to avoid the effect of changing liver glycogen and water storage of ultrasound attenuation.

Data acquisition for the system were obtained in a transverse subcostal section taken for patients just preceding a needle biopsy procedures on their livers. The data from the pathology laboratory were used with the other biochemical, clinical, and other measurements to identify the exact condition of all obtained images.

3. MATERIALS AND METHODS

The steps done to correct different machine settings are:

-Look Up Table (LUT) Correction :

The Post processing curve applied to the image is estimated using the gray level wedge image. If the gray levels in the wedge don't show a linear relation ,we have to correct the image for this non-linearity to create a corrected LUT.

Our algorithm overcome this problem by :

-Getting the gray levels in the image wedge. Storing them in a mapping array which is a one dimensional array, the data is the actual gray level of the image, and the dimension is the ideal gray scale starting from 0 to 255 gray levels.

-Filling the missed gray levels found in the image wedge with the nearest gray levels found, then applying curve-fitting algorithm to get the linear relation between gray levels.

-Using the mapping array to correct the whole image. By, using the gray levels from the image as the index of the corrected mapping array and the data in the mapping array as the new corrected value.

$$ROI(i,j) = WD(ROI(i,j)) \quad (1)$$

Where WD is the wdge array and the ROI the image array.

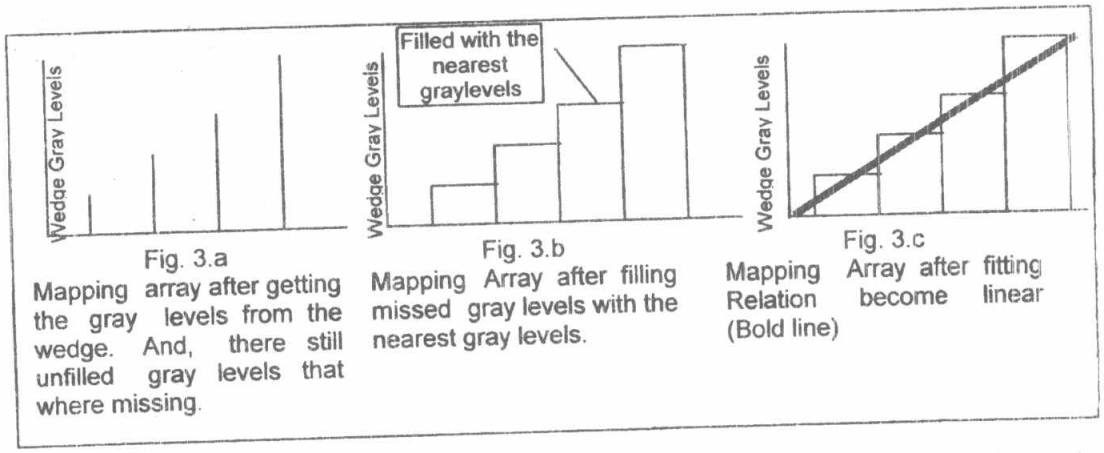

Fig. 3.a Mapping array after getting the gray levels from the wedge. And, there still unfilled gray levels that where missing.

Fig. 3.b Mapping Array after filling missed gray levels with the nearest gray levels.

Fig. 3.c Mapping Array after fitting Relation become linear (Bold line)

By applying the corrected LUT to all pixels in the image, the unreferenced gray levels are eliminated, and then the gray levels in the wedge shows a linear decrease. See figures (6.a-6.b) in results.

-Time-Gain-Control (TGC) Correction :

On most modern clinical instruments, the rate of Time Gain Control (TGC) is variable and under the control of the operator to meet the specific needs of the

application. The penetration depth is divided into several segments and a separate sliding knob determines the rate of TGC increase for each segment.(see fig 4.d) This Time Gain Control (also known as a Time Gain Compensation) helps compensate for the ever decreasing signal strengths from deeper tissues due to the greater attenuation over longer paths. Thus, the gain ramps up at a rate that tends to balance tissue absorption. Fig.4 illustrates some curves of different TGC as a function of depth to compensate tissue losses.

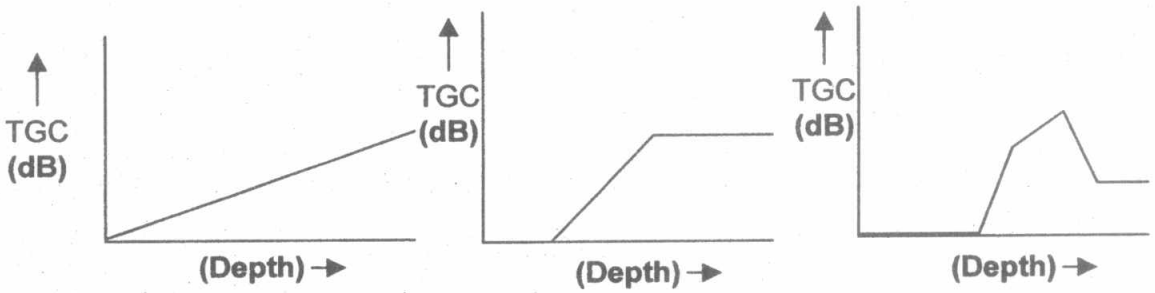

Fig. 4.a *Fig. 4.b* *Fig. 4.c*

In fig. (4.a) a linearly increasing gain curve may be theoretically optimal but is of little usage in practice. At fig. (4.b) it is often desirable to de-emphasize near boundaries and to avoid high amplification of noise at very deep boundaries. Fig. (4.c) shows that if a certain structure at a known distance is to be highlighted. This flexibility allows to avoid giving too much gain to structures close to the transducer, so the gains of the initial segments are set constant and low. Echoes from boundaries much deeper than the region of interest may also be de-emphasized by setting the gain constant there.

In order to release the effect of TGC from the image, our correction step must be taken, the initial segment taken as a standard or referenced segment and the other segments appears like a deviated segments from this symmetrical or referenced segment so we build our algorithm as:

-Interpolate the deviated segments individually by applying the linear interpolation algorithm to get a linear straight line between the 2 knobs in the same segment.

-Detecting the slope of each segments.

-Taking the difference factor (xi) between the referenced segment and the deviated segments.

-Each pixel in the image related to one of those segments are corrected by dividing all the pixels in the Image by the corresponding difference factor

$$G(I,J)=G(I,J)/(xi) \qquad (2)$$

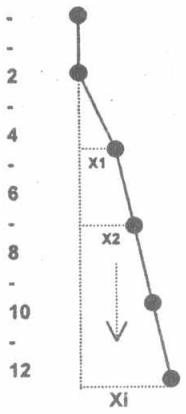

Fig. 4.d

where G(I,J) represents the gray levels values of pixel at position I, J,and (xi) the difference factor between the reference segment and the other segments.(see fig4.d) After the dividing process is done according to the last equation, the effect of the TGC is corrected for the image. So now the data is independent from TGC and according to this correction effect, the values of gray levels in the image well be decreased.

-Correction steps for Diffraction and Focusing

When transmitting an ultrasound signal to a tissue using an ultrasound transducer, the signal interacts with the tissue and the received signal depends on the following parameters:

(i) P(f) the electroacoustic round-trip transfer function of the piezoelctric material of the transducer

(ii) S(f) the average backscattering coefficient of the tissue inhomogenities, which is assumed to be constant in the ROI

(iii) $H'_t(f,r)$, $H'_r(f,r)$ the transfer functions associated with the impulse response function of the transducer at position r in transmission and reception, respectively [9].

The average of many A-scans, from the same medium at various depths is first compensated for attenuation using tissue mimicking phantom or average of normal liver cases. The resultant compensated pulse echo data should be constant, (i.e independent of the distance to the transducer). Deviations from a constant value are persumed to be due to diffraction and focussing effects. A correction curve is given by:

$$D_i = D_1 C_i \exp[-2\mu_{ph} i l] \quad (3)$$

Where μ_{ph} is the phantom attenuation coefficient expressed in neper cm^{-1}, l is the length of the pixel (1/16 to 1/40), D_i is the average of the A scans at depth i, and C_i represents a correction factor . For each pixel i an approximate correction factor is computed. In such a manner a correction function C(x) is computed

Correction is performed by dividing echo amplitude (value of gray levels in the image) from depth x by the value c(x) according to the eq:

$$G(I,J)=G(I,J)/c(x) \quad (4)$$

Where G(I,J) is the gray levels value.

By applying this equation to all pixels in a selected region of interest (selected by the operator) the gray level for sure well be more brightened according to correction of diffraction of transducer,(i.e equalizing the power for all pixels in the ROI).

4.RESULTS

- LUT Correction :-

The original image before correction shown in fig 5.a have a mean gray level 71.58 shown in fig (5.b), the histogram in this fig (5.b) is the histogram of the original image which analyzes the image gray levels.
Fig 5.c illustrates the non-linear relations between the gray levels (the upper part) then this relation becomes linear after correction (lower part).
The next fig (6.a) shows the image after correction but it's not easily to detect the difference after correction by visual inspection for the ultrasound images so we analyze the images using it's histogram and mean gray level by observing the histogram shown in fig 6.b which shows a decrease in mean gray level from 71.58 to 60.45.

- TGC correction :

By using the image after LUT correction and applying the T.G.C correction algorithm to it, fig 7.a shows this image after T.G.C correction. Fig.7.b shows it's histogram which illustrates clearly how gray levels decreased (shifted to the dark region at the left) after correction and the mean gray levels also shifted to 19.02 .

-Diffraction and focusing correction:

Fig 8.a shows the AIUM phantom with a known attenuation, by estimating the diffraction correction curve shown in fig 8.b, this curve will be applied to the image which already corrected using LUT correction and TGC correction (see fig 7.a) we select the ROI by polygon to detect the Region will be corrected.
Fig 9.a shows the image after applying the diffraction correction curve to the selected ROI , the gray levels are shown to be more bright (increasing in gray level) because of the correction effect of diffraction so the power will be distributed for all pixels and attention effect will be corrected.
The histogram in fig 9.b shows the mean gray level (73.68) and the histogram of the image return back to distribute the gray levels for all 256 gray scale.

5.DISCUSSION AND CONCLUSION

We have shown that the steps of correcting the acquired ultrasound image may improve the quality of the image and the image has a minimum dependency on the machine. Thus in image analysis , the textural parameters, histogram and other parameters are independent of the machine.
Extraction of machine independent ultrasound parameters can be used for pattern recognation application, 3D reconstruction and tissue characterization of diffused disease such as in liver ,spleen and kidney.
Porting of a calculated image parameters database from a machine to anther machine can now be easily done using the illustrated correction protocol in this paper.

6. List of figures:

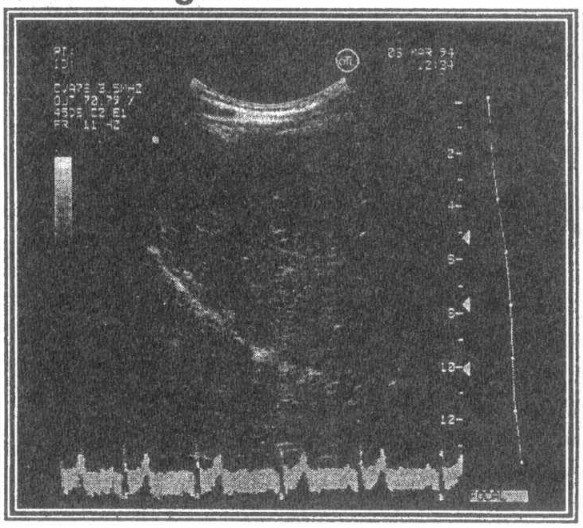

Fig 5.a The original Ultrasound image

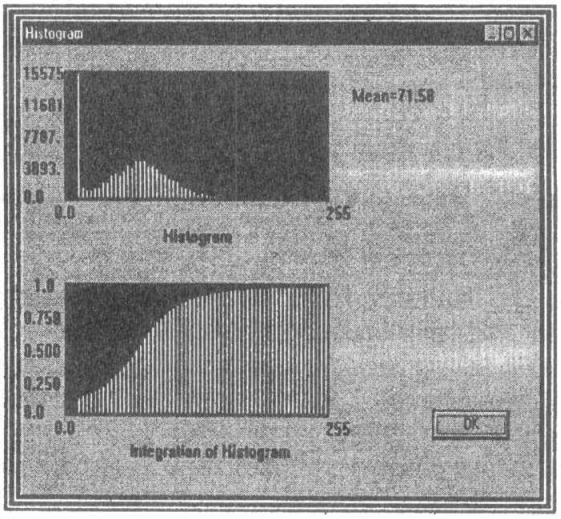

Fig5.b Histogram of the original image

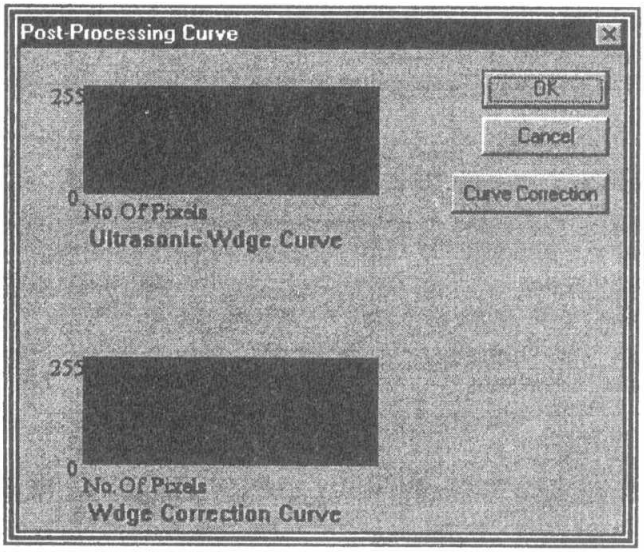

Fig 5.c ultrasound wedge curve before and after LUTcorrection

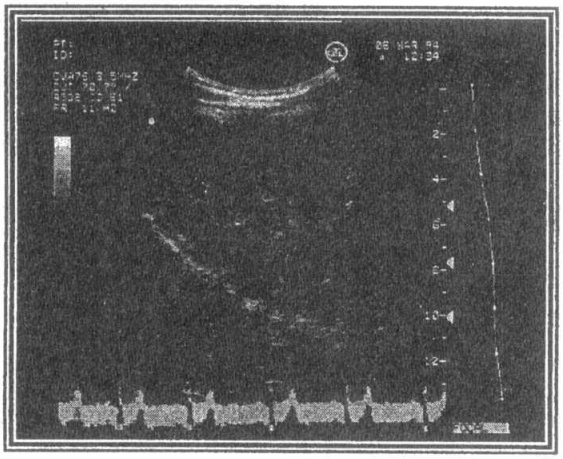

Fig 6.a image after LUT correction

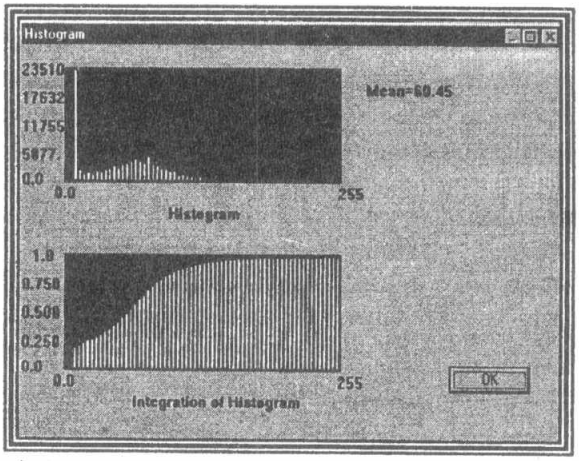

Fig 6.b Histogram of image after LUT orrection

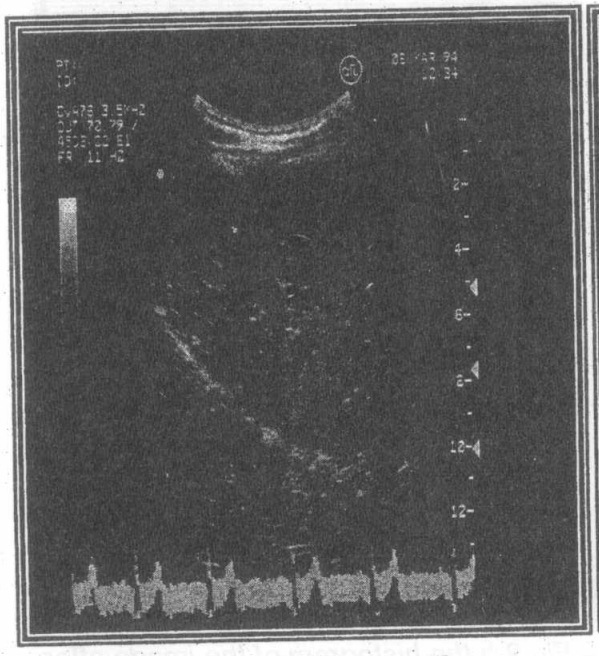

Fig 7.a image after TGC correction.

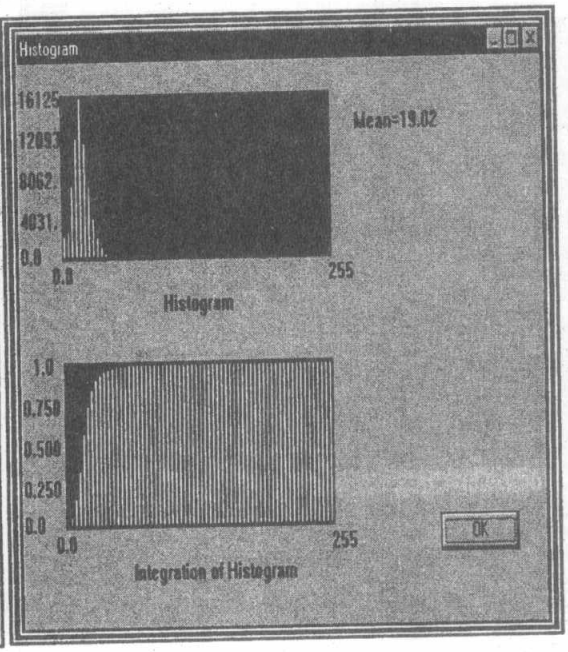

Fig 7.b Histogram of image after TGC correction.

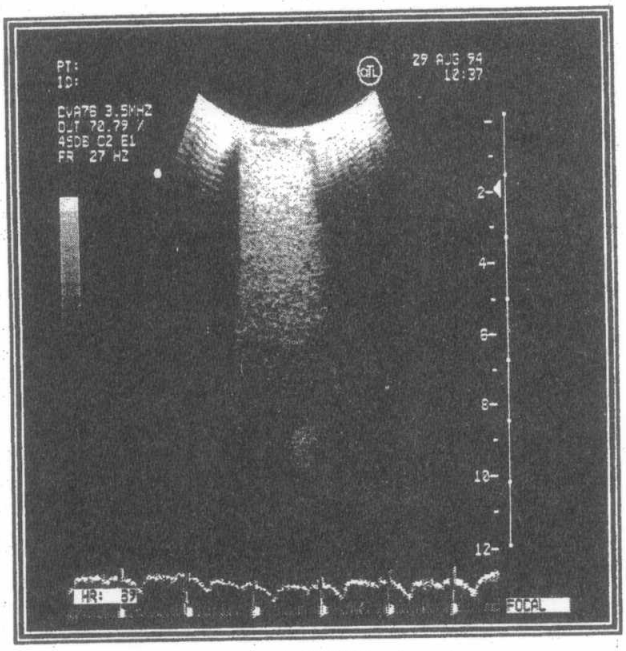

Fig 8.a The original AUIM phantom.

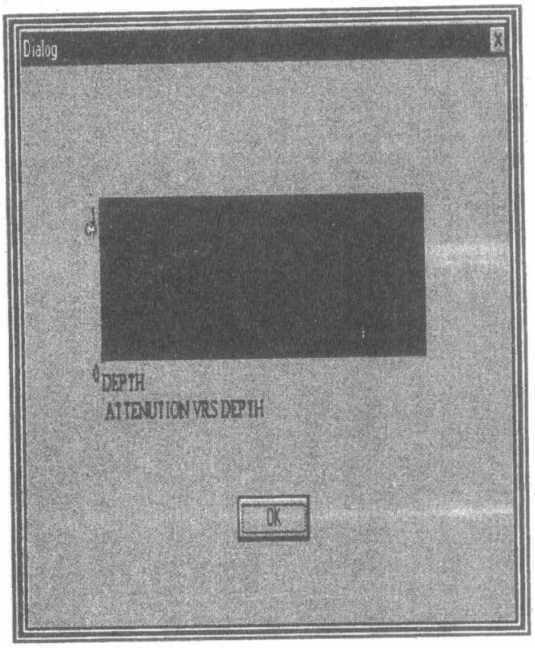

Fig 8.b the Diffraction correction curve estimated by the original phantom with known attenuation.

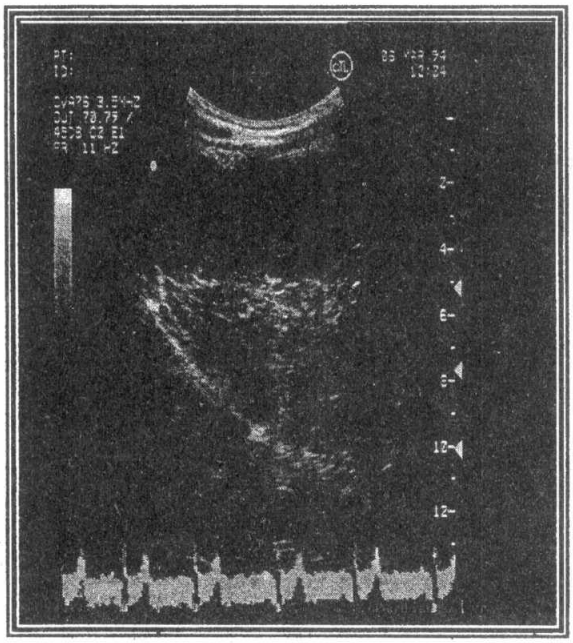

Fig 9.a the image after diffraction and focusing correction

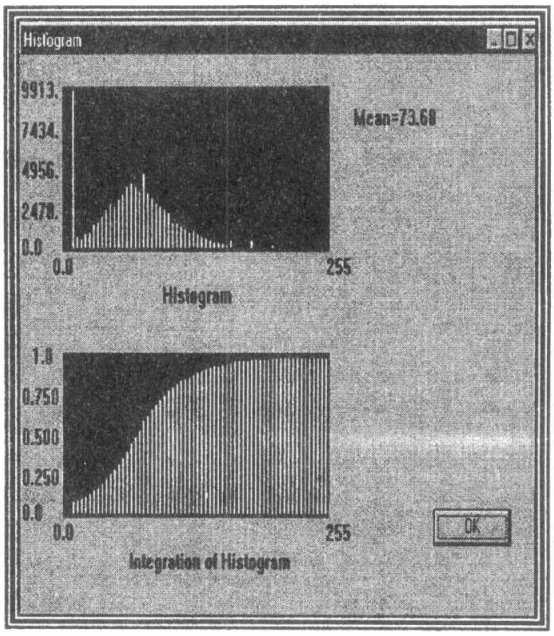

Fig.9.b the histogram of the image after focusing and diffraction correction

ACKNOWLEDGMENT

Prof.Dr. A.M.Youssef is acknowledged for his unlimited help to do this work.

REFERENCES

[1] Y. M. Kadah, A. A. Farag, A. M. Badawi, A. M. Youssef, "Classification algorithms for quantitative tissue characterization of diffuse liver disease from ultrasound images," Trans. of IEEE, Med. Imag., Vol 15, No. 4, August, 1996.

[2] Gosink, B.B., Lemon, S.R., Scheible, W., Leopold, G.R., Accuracy of ultrasonography in diagnosis of hepatocellular disease, AJR.pp.Vol. 133, 19-23, 1979.

[3] Raeth, U., Schlaps, D., Limberg, B., Zuna, I., Lorenz, I., Van Kaick, .G, Lorenz, W.J., Kommerell, B., Diagnostic accuracy of computerized B-scan texture analysis and conventional ultrasonography in diffuse parenchymal and malignant liver disease, J Clin. Ultrasound , 13: 87-99, 1985.

[4] Chung-Ming Wu, Yung-Chang Chen, and Kai-Shang Hsieh, "Texture Features for Classification of Ultrasonic Liver Images.", IEEE Transaction on Medical Imaging, Vol. 11, NO. 2, June 1992.

[5] D. Schlaps, U. Rath, J. F. Volk, I. Zuna, A. Lorentz, K. J. Lehmann, D. Lorentz, G. V. Kaick, W. J. Lorentz, "Ultrasonic tissue characterization using a diagnostic expert system". In bacharadt,S. L. edn. :Information processing in medical imaging, p. 343, Martinus Nijhoff, Dordecht, 1986.

[6] A. M. Badawi, A. M. Youssef, "Effect of Static Compression on the Acoustical and Textural Parameters of the Liver with Correlation to Diffuse Diseases," Annual Meeting of Egy. Society of Gastro. and Egy. Soc. of Ultras., December 1992.

[7]A. M. Badawi, A. M. Youssef, "Tissue Characterization of Diffuse Liver Diseases Using Neural Nets," Annual Meeting of Egy. Soc. of Gastro. and Egy. Soc. of Ultrasonography, December 1992.

[8]Y. M. Kadah, Aly A. Farag, Jacek M. Zurada ,A. M. Badawi, Abou-Bakr M. Youssef, "Quantitative Algorithms for Tissue Characterization of Liver Disease from Ultrasound Images", IEEE Medical imaging journal , Vol 3 , August, 1996

[9]A. M. Badawi, " Quantitative Techniques and Algorithms for Ultrasound Tissue Characterization of Liver Diseases", Ph.D. Faculty of Eng. Cairo Univ.1996.

[10] Jaffer CC, Harris DJ: Sonographics tissue: Influence of transducer focussing pattern. Am J Roentegenol 135:343,1980.

[11] Wells PNT, Halliwell M: Speckle in ultrasonic imaging
Ultrasonics 19:225, 1981.